INTERNATIONAL JOURNAL OF OCCUPATIONAL
SAFETY AND ERGONOMICS (*JOSE*) 2003, VOL. 9, NO. 1, 37–56

Enhancement of Drilling Safety and Quality Using Online Sensors and Artificial Neural Networks

Tien-I Liu
Akihiko Kumagai
Chongchan Lee

Department of Mechanical Engineering,
California State University,
Sacramento, USA

Cutting force sensors and neural networks have been used for the occupational safety of the drilling process. The drill conditions have been online classified into 3 categories: safe, caution, and danger. This approach can change the drill just before its failure. The inputs to neural networks include drill size, feed rate, spindle speed, and features that were extracted from drilling force measurements. The outputs indicate the safety states. This detection system can reach a success rate of over 95%. Furthermore, the one misclassification during online tests was a one-step ahead pre-alarm that is acceptable from the safety and quality viewpoint. The developed online detection system is very robust and can be used in very complex manufacturing environments.

drilling safety online sensors artificial neural networks

1. INTRODUCTION

Workers consider their safety as the very first priority for their professional goals as shown in Table 1 (National Safety Workplace Institute [NSWI], 1992). According to the research of the National Institute for Occupational

This research is partially sponsored by the California State Funded Research, Scholarly and Creative Activity Award. The authors would like to express their appreciation to Mr. K.S. Anantharaman for conducting the drilling experiments.

Correspondence and requests for offprints should be sent to T.I. Liu, Department of Mechanical Engineering, California State University, Sacramento, CA 95819, USA. E-mail: <liut@csus.edu>.

Safety and Health, one of the most important sources of fatal injuries is machines (Etherton & Myers, 1990). To avoid the safety problems in the manufacturing processes, a very reliable online prediction of tool conditions is necessary (Etherton & Myers, 1990; Millard, 1991; National Safety Council, 1992; NSWI, 1992; Niu, Wong, Hong, & Liu, 1998; Roth & Pandit, 1999; Sata, Matsushima, Nagakura, & Kono, 1973). An effective tool condition classification system can eliminate the risk of injury during machine operation. Successful online tool condition monitoring is also beneficial for productivity because tool failure accounts for 8% of machine tool down time (Altintas, 1992; Niu et al., 1998; Park & Ulsoy, 1993a, b; Purushothaman & Srinivasa, 1994; Subramanian & Cook, 1977). In addition, online diagnosis of tool condition can improve product quality and reduce product costs (Liu, Lee, & Wang, 2001; Liu, Wang, and Lee, 2000; Ramamurthi & Hough, 1993; Rangwala & Dornfeld, 1990; Society of Manufacturing Engineers, 1976, 1984; Xie, Bayoumi, & Kendall, 1990).

TABLE 1. Employee Goals for Corporate Performance, 1989 (National Safety Workplace Institute, 1992)

Rank	Goal
1	Safe working condition
2	Ethical corporation behavior
3	Good benefits
4	Honest company communications
5	Respectful treatment
6	Good equipment and resources
7	Competent top management
8	Quality products and services
9	Good pay
10	Comfortable working condition

The National Electronic Injury Surveillance System (NEISS) database provides the ranks of severity and frequency of injuries for different types of machines. The product of the sum of severity scores and the frequency of injury for the USA was computed for various kinds of machines in the NEISS database. The ranked order of the severity using this product as an index is shown in Table 2 (Etherton & Myers, 1990).

TABLE 2. Rank Order of Severity by Frequency Products for Injuries Involving Manufacturing Machines Only, Hospital Emergency Rooms in the USA, 1985 (Etherton & Myers, 1990)

Manufacturing Machines	Rank of Severity by Frequency Product
Presses	1
Shears, slitters, slicers	2
Saws	3
Buffers, grinders	4
Drilling, boring, turning	5
Rolls	6
Tumblers, and so forth	7
Casting, forging, welding	8
Metal lathes	9

The most common hazards in drilling operations are (National Safety Council, 1992)

- being struck by a broken drill;
- using dull drills;
- being struck by flying metal chips;
- contacting the rotating spindle or tool;
- being struck by insecurely clamped work;
- catching hair, clothing, or gloves in the revolving parts;
- sweeping chips, or trying to remove long, spiral chips, by hand.

Because drilling operation is one of the major sources of fatal injuries as indicated in Table 2, the development of an online drill condition detection system is essential for occupational safety.

In this work, an intelligent online drill failure detection system has been developed. Cutting forces, that is, thrust and torque, have been chosen for the monitoring of drill conditions because they are closely related to the drilling process and give very good indication of drill states. Cutting forces are very sensitive to the changes in drilling conditions. Back propagation neural networks have been used for the classification of drill states. The inputs have been extracted from cutting forces and the outputs are drill conditions.

Researchers have developed drill condition classification systems (Barker, Klutke, & Hinich, 1993; Govekar & Grabec, 1994; Li, Lau, & Zhang, 1992; Liu & Anantharaman,1994; Liu, Chen, & Anantharaman, 1998; Liu, Chen, & Ko, 1994; Subramanian & Cook, 1977; Thangaraj & Wright, 1988). These systems can classify drills into two categories: usable or failure. The drawback

of this two-category classification is that it may be too late when the drill failure has been detected. In other words, an operator may still be exposed to a dangerous working environment. This kind of online drill condition classification is not satisfactory for occupational safety. In this work, three drill conditions, that is, safe, caution, and danger, are detected. This system can detect a potentially unsafe condition so that corrective actions can be taken in advance.

In section 2, artificial neural networks are briefly described. In section 3, experimentation and feature extraction are discussed. The learning process of back propagation neural networks, online detection of drill conditions, and discussions are given in section 4. Section 5 gives the conclusions of this research.

2. NEURAL NETWORK

Figure 1 shows the structure for a typical three-layered, back propagation neural network. The bottom layer of neurons is the input layer. The neurons in the input layer receive inputs. The neurons of the input layer send information to the neurons in the hidden layer, which is between the input and output layers. The top layer is the output layer, which provides the output. Each

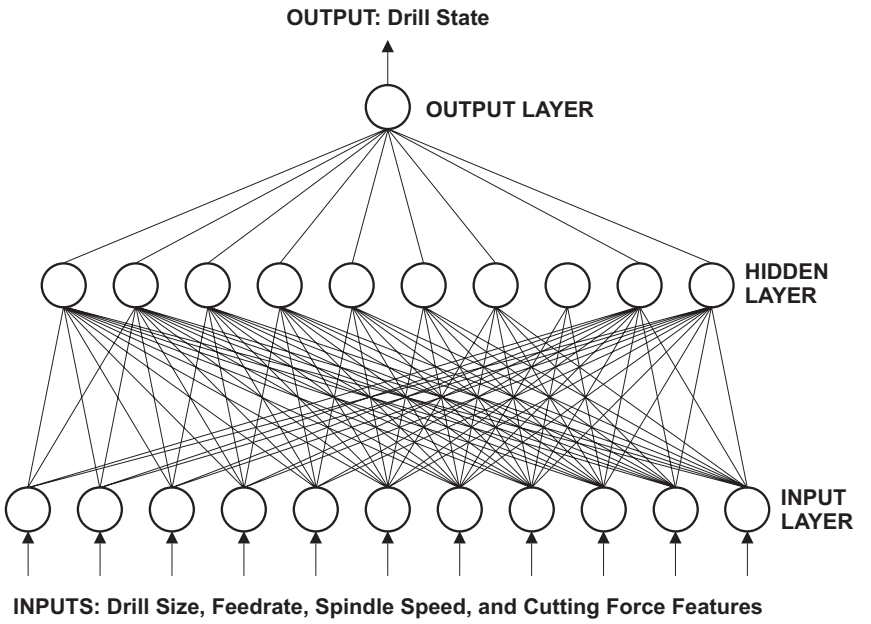

Figure 1. The structure of an $11 \times 10 \times 1$ back propagation neural network.

neuron is connected to every neuron in the layer above and below, but they are not connected to other neurons in the same layer (He, Zhang, Lee, and Liu, 2001; Kumagai, Hozian, & Kirkland, 2000; Liu, 1998).

All the raw data are normalized between 0.1 and 0.9 as shown in the following equation:

$$a_i = \frac{0.8}{r_{max} - r_{min}}(r_i - r_{min}) + 0.1, \quad (1)$$

where a_i is the normalized data, r_{max} and r_{min} are the maximum and minimum values of the raw data, respectively. And r_i is the i-th raw input data.

The outputs of neurons on the input layer reach the j-th neuron on the next layer and become its input as follows:

$$S_j = \sum_{i=1}^{n} a_i \cdot W_{ji}, \quad (2)$$

where a_i is the output value from the i-th neuron of the input layer and n is the number of neurons of the input layer. And w_{ji} is the weight between the i-th neuron on the input layer and the j-th neuron on the next layer.

The output of the j-th neuron is shown below in Equation 3:

$$f(S_j) = \frac{1}{1 + \exp(-\sum a_i \cdot W_{ji})}. \quad (3)$$

The neuron on the output layer computes its output. In the learning process, the computed output is compared with the desired output. The difference propagates backwards. Then the weights of all of the interconnections are adjusted (Sereno, 1993). The error of the j-th neuron on the output layer is obtained with

$$\delta_j = (d_j - a_j) \cdot f'(s_j), \quad (4)$$

where d_j is the desired output value for the j-th neuron, a_j is the computed output value for the j-th neuron, $f'(s_j)$ is the derivative of the sigmoid function f with respect to s_j, and s_j is the weighted sum of inputs to the j-th neuron. The error of the j-th neuron on the hidden layer is calculated with Equation 5:

$$\delta j = \left\{ \sum_k \delta_k \, W_{kj} \right\} \cdot f'(s_j). \quad (5)$$

The back propagation rule updates the weights according to Equation 6:

$$\Delta W_{ji} = \alpha \cdot \delta_j \cdot a_i, \tag{6}$$

where ΔW_{ji} is the change of the weight from the i-th neuron to the j-th neuron, α is the learning rate.

Smoothing technique can be used to improve the learning process. It is expressed by Equation 7:

$$\Delta W_{ji}^{new} = (1-\beta)\,\alpha \cdot \delta_j \cdot a_i + \beta \cdot \Delta W_{ji}^{old}. \tag{7}$$

The error calculation and weight updating process continue until the neural network computes an output that is close to the desired output. Once the learning process is completed, the neural network can be utilized for online applications.

3. EXPERIMENTAL PROCEDURE AND FEATURE EXTRACTION

3.1. Experimental Setup

The drilling experiments were carried out on a Bridgeport (USA) 3-axis CNC milling machine. A Kistler (Switzerland) 9271A piezoelectric dynamometer was used to measure the cutting forces, namely, thrust and torque. Two Kistler model 5004 charge amplifiers with a 470 Hz anti-aliasing low pass

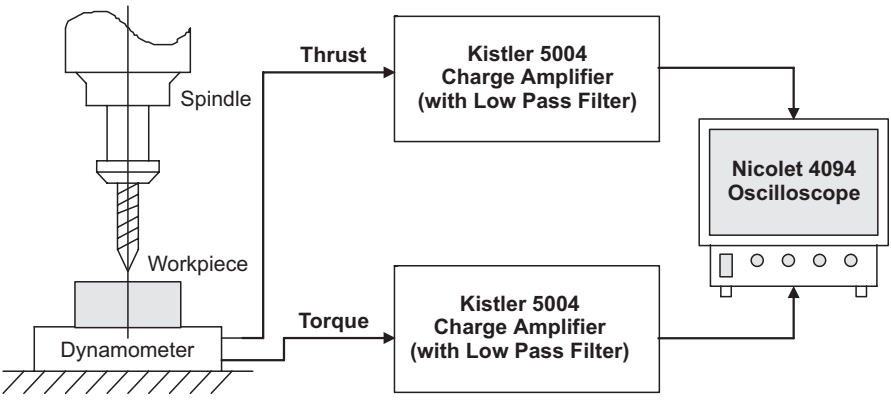

Figure 2. A schematic diagram of the experimental setup.

filter were used for the amplification of the measured signals. Then the signals were input and displayed on a Nicolet (USA) model 4094 oscilloscope. The sampling frequency of the measurements was 1000 Hz, which avoids aliasing. The schematic diagram for this experimental setup is shown in Figure 2.

The work material used in this work was 303 stainless steel. The size, hardness, and chemical composition of the work material are described in Table 3. All the drilling experiments were conducted until the drill was broken or completely worn-out. High speed steel (HSS) twist drills were used during the tests. Three different drill sizes, three different feedrates, and four different spindle speeds were used in this experiment.

TABLE 3. Size, Hardness, and Chemical Composition of the Work Material

Work material	303 stainless steel	
Hardness	175 BHN	
Composition	Carbon	0.15%
	Chromium	18%
	Manganese	2%
	Molybdenum	0.6%
	Nickel	9%
	Phosphorus	0.2%
	Silicon	1%
	Sulfur	0.15 %
Length	304.8 mm (12.0 in.)	
Width	25.4 mm (1.0 in.)	
Height	25.4 mm (1.0 in.)	

Data sets from the drilling experiments were utilized for the training of neural networks. Then, online tests were performed for the classification of drill conditions. Table 4 gives a summary of various drilling experiments.

TABLE 4. Summary of Drilling Experiments

Purpose	Drill Size, in mm (in.)	Feed Rate, in mm/s (in./min)	Spindle Speed, in rpm	Number of Holes Drilled
Learning process	6.350 (1/4)	0.330 (7.8)	750	13
	4.762 (3/16)	0.305 (7.2)	1030	6
Online tests	6.350 (1/4)	0.330 (7.8)	900	14
	3.175 (1/8)	0.228 (5.4)	1800	10

3.2. Feature Extraction

In order to enhance the reliability of the online sensory system, it is essential to select the best combination of parameters. Thrust and torque give very important information about drill conditions. Therefore, online drill failure detection is possible using thrust and torque signals. Signal processing techniques were employed to obtain various parameters from thrust and torque signals. The features extracted from thrust and torque signals are described in the following:

1. Average thrust (or torque)
   This value is defined by

$$\overline{T} = \frac{\sum_{i=1}^{n} T_i}{n}, \tag{8}$$

   where $\overline{T}$ is the average value of thrust (or torque), T_i is the value of the i-th thrust (or torque), n is the number of thrust (or torque) values.
2. Peak thrust (or torque)
   Peak of thrust (or torque) is simply the maximum value of each thrust (or torque) measurement in the drilling experiments.
3. RMS thrust (or torque)
   This value indicates the power consumption during drilling and is defined by

$$\text{RMS} = \sqrt{\frac{\sum_{i=1}^{n} T_i^2}{n}}. \tag{9}$$

4. Area under thrust (or torque) versus time curve
   This value is integral of the area under thrust (or torque) curve with respect to time and is very sensitive to the change of drill condition. This is obtained with

$$\text{Area} = \int_0^t T\,dt, \tag{10}$$

   where T is the thrust (or torque), t is the time taken for each hole drilled.

In this work, a total of 11 features, including drill size, feed rate, spindle speed, thrust and torque are input to neural networks. Table 5 shows all 11 features for the classification of drill conditions.

TABLE 5. List of 11 Features for Online Detection of Drill Conditions

Number	Feature
1	Drill size
2	Feedrate
3	Spindle speed
4	Average thrust
5	RMS thrust
6	Peak thrust
7	Thrust versus time area
8	Average torque
9	RMS torque
10	Peak torque
11	Torque versus time area

4. ONLINE DETECTION OF DRILL CONDITIONS

Online detection of drill conditions has been performed. Various structures of neural networks have been used. Neural networks have been trained in the learning process. They are then used for online tests. The effects of different parameters, such as weights, learning rates, and smoothing factors on the performance of an online drill failure detection system have been evaluated and compared.

4.1. Learning Process

Two data sets were used for the training of neural networks. The drill size, feedrate, and spindle speed of these two data sets were quite different. Two drill sizes, 6.350 mm (1/4 in.) and 4.762 mm (3/16 in.), were used. The first 13 training data were obtained with a spindle speed of 750 rpm and a feedrate of 0.330 mm/s (7.8 in./min). Another 6 training data were taken with the drilling conditions: spindle speed 1030 rpm and feedrate 0.305 mm/s (7.2 in./min). The raw data for the learning process are shown in Table 6.

All the numerical data were normalized to be between 0.1 and 0.9. They were then put into neural networks. The learning rate used was 0.9. The initial weights were randomly assigned between –0.8 and 0.8. No smoothing factor was used. The learning process stopped after 15,500 iterations.

The neural networks' outputs indicate the drill states. Drill states are classified into three categories according to their output values. The three

TABLE 6. Raw Data in the Learning Process

Test Condition	No. of Hole	Average Thrust (mv)	RMS Thrust (mv)	Peak Thrust (mv)	Thrust Time Area (mv-s)	Average Torque (mv)	RMS Torque (mv)	Peak Torque (mv)	Torque Time Area (mv-s)
Drill diameter	1	259.40	260.50	306.70	36000	47.90	48.50	74.40	6900
6.350 mm	2	271.10	269.80	313.60	37000	49.30	49.20	75.20	7100
(1/4 in.)	3	271.90	271.20	376.60	36300	52.60	53.30	76.20	7200
Feed rate	4	274.10	277.60	326.50	37600	48.50	50.40	84.20	7300
0.330 mm/s	5	280.10	280.30	333.10	37000	52.80	53.30	96.80	7600
(7.8 in./min)	6	283.50	283.70	326.50	38500	50.70	51.10	75.80	7200
Spindle speed	7	271.40	271.70	321.10	43000	52.40	53.60	104.80	8400
750 rpm	8	347.90	344.60	418.70	49000	64.78	65.10	108.20	9300
	9	371.60	369.30	454.00	51300	74.30	74.60	146.00	10600
	10	369.70	368.20	435.60	50900	73.11	73.00	154.20	10200
	11	373.90	375.30	440.10	50700	81.17	83.60	184.00	12500
	12	361.40	361.30	507.50	49000	72.40	73.60	178.60	11000
	13	454.12	467.30	807.90	61200	103.40	122.00	604.80	17700
Drill diameter	1	179.30	169.31	298.70	23900	22.90	23.23	39.25	3300
4.762 mm	2	183.45	170.78	307.60	24800	23.00	24.56	56.00	3500
(3/16 in.)	3	189.78	190.75	325.60	25800	24.60	25.96	58.05	3700
Feed rate	4	191.68	190.44	339.50	25500	25.48	27.20	69.34	3600
0.305 mm/s	5	193.38	195.45	373.40	26400	26.40	28.06	77.13	3600
(7.2 in./min)	6	201.50	200.45	451.10	29100	33.30	39.36	167.23	6100
Spindle speed 1030 rpm									

categories and the desired output values in the learning process are shown in Table 7. Category I is the safe state. The drill is usable and safe. It definitely offers safe conditions for the operator. Category II is the caution state. When the drill was used to make the penultimate hole, it was chosen as the caution state. It indicates that the machine should be stopped and the drill should be replaced even though the drill is still usable. Category III is the danger state. It shows that the drill is about to break or worn out as indicated by loud noise or inability to cut.

TABLE 7. Assigned Output Values for Different Drill States in the Learning Process

Category	Drill State	Desired Output Value
I	safe	0.234[a]
I	caution	0.501[b]
III	danger	0.768[c]

Notes. a—the mid-value of 0.100–0.367 for category I, b—the mid-value of 0.368–0.634 for category II, c—the mid-value of 0.635–0.900 for category III.

4.2. Online Detection of Drill Conditions

Once neural networks have been trained, they can be applied for online tests. The online test conditions are very different from the drilling conditions in the learning process so as to evaluate the generalization capability of neural networks. Two tests with different drill sizes and drilling conditions were performed. For the first 14 tests, the drilling experiments were conducted using a 6.350 mm (1/4 in.) diameter drill with a spindle speed of 900 rpm and a feedrate of 0.330 mm/s (7.8 in./min). For another 10 tests, the drilling operations were performed using a 3.175 mm (1/8 in.) diameter drill with a spindle speed of 1800 rpm and a feedrate of 0.228 mm/s (5.4 in./min). The drill states were classified online into three categories according to the following output values:

- If the output value is in the range of 0.100–0.367, then the drill belongs to Category I—Safe;
- If the output value is in the range of 0.368–0.634, then the drill belongs to Category II—Caution;
- If the output value is in the range of 0.635–0.900, then the drill belongs to Category III—Danger.

TABLE 8. Raw Data for Online Tests

Test Condition	No. of Hole	Average Thrust (mv)	RMS Thrust (mv)	Peak Thrust (mv)	Thrust Time Area (mv-s)	Average Torque (mv)	RMS Torque (mv)	Peak Torque (mv)	Torque Time Area (mv-s)
Drill diameter	1	289.50	280.60	326.30	36000	49.30	49.20	74.20	6800
6.350 mm	2	291.50	289.70	333.70	36300	52.50	53.30	76.20	7200
(1/4 in.)	3	291.80	291.30	394.60	37600	50.30	50.40	84.20	6900
Feed rate	4	294.30	297.40	350.50	37800	53.40	53.30	96.80	7600
0.330 mm/s	5	305.10	300.10	373.10	38500	51.70	51.10	95.80	7200
(7.8 in./min)	6	308.30	303.50	391.10	43000	52.30	53.60	104.80	8400
Spindle speed	7	291.90	391.90	420.50	49000	54.80	65.10	108.20	9300
900 rpm	8	367.90	364.80	440.10	51300	74.10	74.60	146.00	10600
	9	389.80	389.50	461.20	50900	75.10	73.00	154.20	10200
	10	393.90	388.40	479.30	51500	82.20	83.60	184.00	12500
	11	381.40	395.50	520.10	49000	83.50	78.60	178.60	11000
	12	425.60	381.50	535.50	51800	103.50	122.60	288.50	17000
	13	465.60	468.70	604.60	52800	109.50	135.40	425.60	18900
	14	495.30	498.10	829.70	54500	111.80	158.80	608.80	19900
Drill diameter	1	69.80	69.72	92.16	0.138	17.22	17.70	62.72	0.0070
3.175 mm	2	77.16	77.80	105.20	0.156	18.41	18.30	63.40	0.0110
(1/8 in.)	3	93.90	93.90	110.16	0.191	22.53	22.60	69.12	0.0110
Feed rate	4	74.90	74.90	105.70	0.153	20.44	21.44	67.36	0.0125
0.228 mm/sec	5	83.56	83.44	103.20	0.165	17.51	17.90	105.60	0.0137
(5.4 in./min)	6	76.60	76.50	98.90	0.155	32.13	32.80	78.80	0.0175
Spindle speed	7	76.70	76.80	94.90	0.153	22.52	22.60	82.04	0.0250
1800 rpm	8	79.50	81.20	188.80	0.180	28.91	19.14	82.56	0.0180
	9	86.16	86.00	146.40	0.168	24.71	25.30	86.56	0.0280
	10	96.40	87.50	198.40	0.183	37.12	37.76	163.07	18900

Notes. Weight (W): randomly assigned between –0.8 and 0.8; learning rate (α): 0.9; training iterations: 15,500; smoothing factor (β): 0.

TABLE 9. Output Values of Various Neural Network Structures for Online Tests

Network Structure	No. of Hole	11 × 2 × 1	11 × 4 × 1	11 × 6 × 1	11 × 8 × 1	11 × 10 × 1	11 × 12 × 1	Drill Condition
Online test I	1	0.183	0.169	0.168	0.172	0.181	0.179	safe
	2	0.188	0.175	0.172	0.181	0.188	0.190	safe
	3	0.250	0.244	0.238	0.250	0.264	0.267	safe
	4	0.219	0.205	0.202	0.212	0.223	0.224	safe
	5	0.241	0.221	0.216	0.220	0.240	0.239	safe
	6	0.257	0.246	0.243	0.247	0.266	0.267	safe
	7	0.262	0.271	0.223	0.272	0.268	0.293	safe
	8	0.247	0.238	0.237	0.249	0.255	0.260	safe
	9	0.248	0.234	0.234	0.248	0.258	0.255	safe
	10	0.296	0.278	0.279	0.290	0.295	0.300	safe
	11	0.327	0.322	0.316	0.350	0.347	0.353	safe
	12	0.399*	0.366	0.379*	0.369*	0.356	0.383*	safe
	13	**0.549**	**0.488**	**0.482**	**0.478**	**0.472**	**0.476**	**caution**
	14	***0.857***	***0.834***	***0.829***	***0.813***	***0.822***	***0.811***	***danger***
Online test II	1	0.273	0.245	0.229	0.259	0.262	0.223	safe
	2	0.282	0.254	0.238	0.271	0.275	0.235	safe
	3	0.279	0.248	0.234	0.275	0.277	0.238	safe
	4	0.289	0.263	0.246	0.285	0.285	0.249	safe
	5	0.330	0.291	0.277	0.311	0.326	0.277	safe
	6	0.283	0.264	0.248	0.304	0.290	0.269	safe
	7	0.292	0.263	0.248	0.278	0.289	0.252	safe
	8	0.411*	0.397*	0.383*	0.445*	0.448*	0.412*	safe
	9	**0.354***	**0.329***	**0.312***	**0.368**	**0.368**	**0.336***	**caution**
	10	***0.819***	***0.755***	***0.751***	***0.774***	***0.788***	***0.830***	***danger***

Notes. *—a misclassification; weight (W): randomly assigned between –0.8 and 0.8; learning rate (α): 0.9; training iterations: 15,500; smoothing factor (β): 0.

The raw data for the online tests are shown in Table 8. Various neural network structures have been used during those tests. The outputs of several neural network structures are shown in Table 9. The comparison of the success rate of all the neural networks used in the online tests is shown in Table 10 and Figure 3.

TABLE 10. Comparison of the Success Rate of Different Neural Network Structures for Online Tests

Network structure	$11 \times 2 \times 1$	$11 \times 4 \times 1$	$11 \times 6 \times 1$	$11 \times 8 \times 1$	$11 \times 10 \times 1$	$11 \times 12 \times 1$
Success rate (%)	87.5	91.7	87.5	91.7	95.8	87.5
Network structure	$11 \times 14 \times 1$	$11 \times 16 \times 1$	$11 \times 18 \times 1$	$11 \times 20 \times 1$	$11 \times 22 \times 1$	$11 \times 24 \times 1$
Success rate (%)	91.7	87.5	87.5	91.7	91.7	91.7
Network structure	$11 \times 26 \times 1$	$11 \times 28 \times 1$	$11 \times 30 \times 1$	$11 \times 32 \times 1$	$11 \times 34 \times 1$	$11 \times 36 \times 1$
Success rate (%)	95.8	91.7	95.8	91.7	95.8	91.7
Network structure	$11 \times 38 \times 1$	$11 \times 40 \times 1$	$11 \times 50 \times 1$	$11 \times 60 \times 1$	$11 \times 70 \times 1$	$11 \times 100 \times 1$
Success rate (%)	95.8	95.8	91.7	91.7	83.3	91.7

Notes. Initial weight vector (W): randomly assigned between –0.8 and 0.8; learning rate: 0.9; training iterations: 15,500; smoothing factor (β): 0.

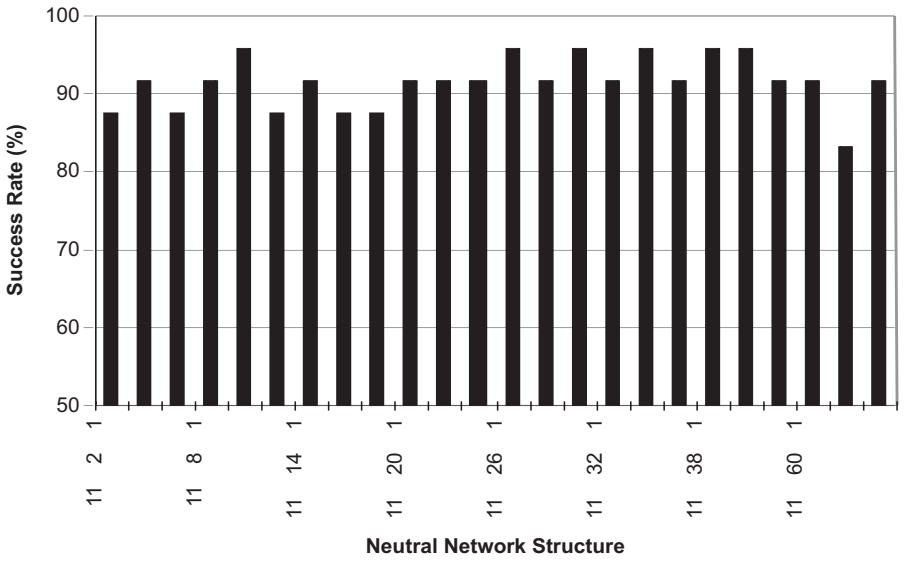

Figure 3. Comparison of the success rate of different neural network structures.

The neural network structure of 11 × 10 × 1 yields the best result. Online drill condition classification can achieve a success rate of over 95%. Furthermore, the one misclassification is a one-step ahead pre-alarm of drill failure, which is acceptable both from an operational safety and product quality viewpoint.

4.3. Comparison and Discussions

After the 11 × 10 × 1 neural network has been selected as the best neural network structure for the online drill condition detection, the influence of the initial weight vector (W), the learning rate (α), and the smoothing factor (β) on its performance has been investigated. In the learning process, the value of the weights were randomly assigned between –0.1 and 0.1, between –0.2 and 0.2, and so forth. The learning rate was assigned to be 0.1, 0.15, 0.2, and so forth. The smoothing factor was assigned to be 0.1, 0.2, 0.3, and so forth. The success rate versus the initial weight vector, the learning rate, and the smoothing factor for online tests using an 11 × 10 × 1 neural network are shown in Tables 11, 12 and 13, respectively. They are also shown in Figures 4, 5 and 6, respectively. The 11 × 10 × 1 neural network has the best performance when the initial weights are randomly assigned from –0.8 to 0.8, from –0.9 to 0.9, from –1.0 to 1.0, or from –1.1 to 1.1. This neural network has the best performance when the learning rate is 0.85 or 0.9. Also, it has the best performance when the smoothing factor is 0, 0.8, or 0.9.

TABLE 11. The Success Rate of an 11 × 10 × 1 Neural Network With Various Initial Weights (W) for Online Tests

Initial weight (W)	–0.1– 0.1	–0.2–0.2	–0.3–0.3	–0.4–0.4	–0.5–0.5
Success rate (%)	83.3	83.3	87.5	87.5	87.5
Initial weight (W)	–0.6–0.6	–0.7–0.7	–0.8–0.8	–0.9–0.9	–1.0–1.0
Success rate (%)	87.5	87.5	95.8	95.8	95.8
Initial weight (W)	–1.1–1.1	–1.2–1.2	–1.3–1.3	–1.4–1.4	–1.5–1.5
Success rate (%)	95.8	91.7	91.7	91.7	91.7
Initial weight (W)	–2.0–2.0	–3.0–3.0	–4.0–4.0		
Success rate (%)	91.7	87.5	58.3		

Notes. Network structure: 11 × 10 × 1; learning rate (α): 0.9; training iteration: 15,500; smoothing factor (β): 0.

TABLE 12. The Success Rate of an 11 × 10 × 1 Neural Network With Various Learning Rates (α) for Online Tests

Learning rate (α)	α = 0.10	α = 0.15	α = 0.20	α = 0.25	α = 0.30	α = 0.35
Success rate (%)	62.5	62.5	62.5	62.5	62.5	62.5
Learning rate (α)	α = 0.40	α = 0.45	α = 0.50	α = 0.55	α = 0.60	α = 0.65
Success rate (%)	62.5	75.0	87.5	87.5	87.5	91.7
Learning rate (α)	α = 0.70	α = 0.75	α = 0.80	α = 0.85	α = 0.90	α = 0.95
Success rate (%)	91.7	91.7	91.7	95.8	95.8	91.7
Learning rate (α)	α = 1.00	α = 1.05	α = 1.10	α = 1.15	α = 1.20	
Success rate (%)	91.7	91.7	91.7	91.7	91.7	

Notes. Network structure: 11 × 10 × 1; weight (W): randomly assigned between –0.8 and 0.8; training iteration: 15,500; smoothing factor (β): 0.

TABLE 13. The Success Rate of an 11 × 10 × 1 Neural Network With Various Smoothing Factors (β) for Online Tests

Smoothing factor (β)	β = 0	β = 0.1	β =0.2	β = 0.3	β = 0.4
Success rate (%)	95.8	91.7	91.7	91.7	91.7
Smoothing factor (β)	β = 0.5	β = 0.6	β = 0.7	β = 0.8	β = 0.9
Success rate (%)	91.7	91.7	91.7	95.8	95.8

Notes. Network structure: 11 × 10 × 1; weight (W): randomly assigned between –0.8 and 0.8; training iteration: 15,500; learning rate (α): 0.9.

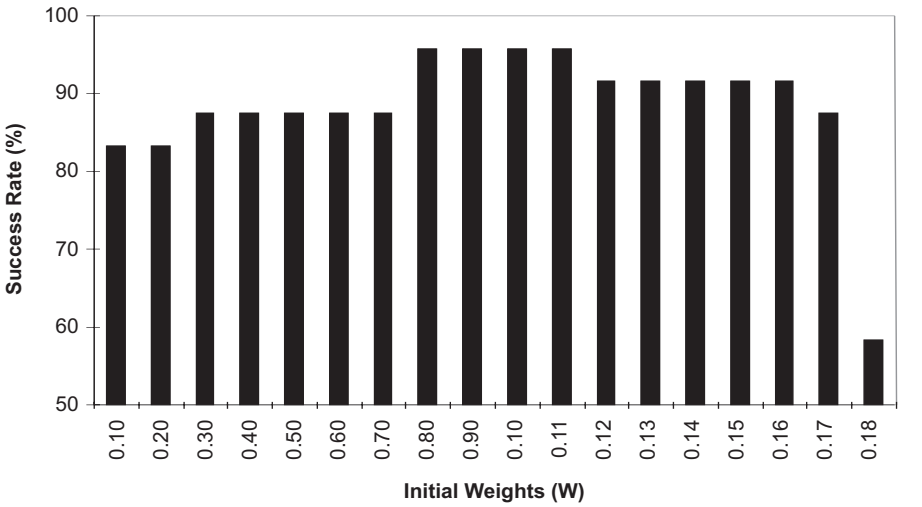

Figure 4. The success rate of an 11 × 10 × 1 neural network with various initial weights (W) for online tests.

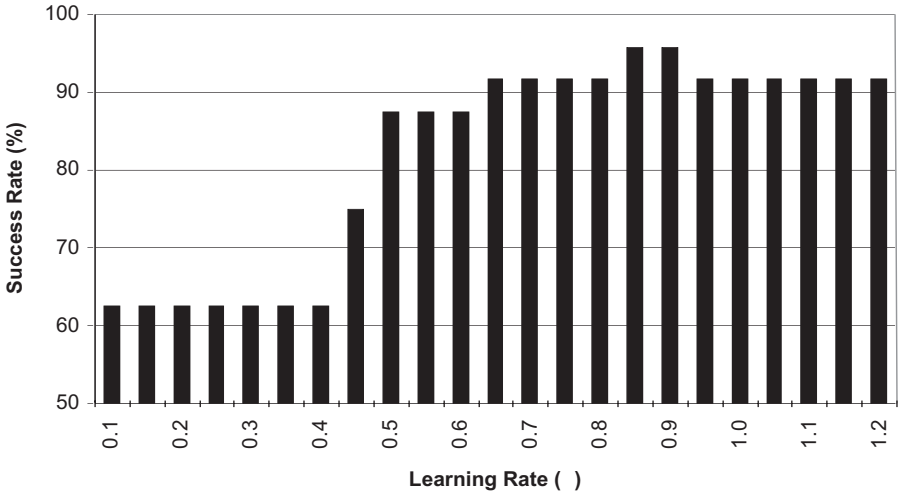

Figure 5. The success rate of an 11 × 10 × 1 neural network with various learning rates (α) for online tests.

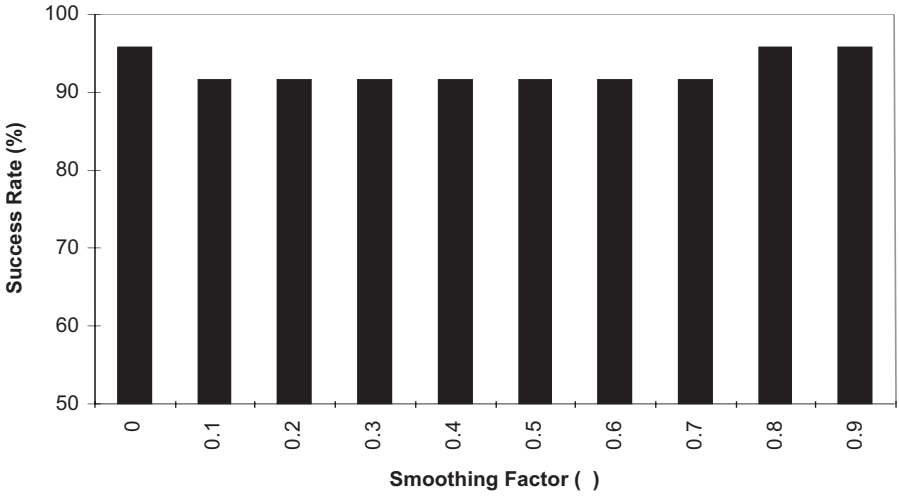

Figure 6. The success rate of an 11 × 10 × 1 neural network with various smoothing factors (α) for online tests.

5. CONCLUSIONS

Based on the descriptions in previous sections, the following conclusions can be drawn:

1. Neural networks have been used successfully for the online classification of drill conditions into three categories: safe, caution, and danger. This

3-category classification can guarantee drill change before drill failure happens. Therefore, it is very beneficial to occupational safety and product quality.

2. The success rate of the online detection system depends on the structure of neural networks. An increase in the number of neurons does not necessarily increase the success rate.
3. An $11 \times 10 \times 1$ neural network yields the best results. It can reach a success rate of over 95% for online recognition of drill states. Furthermore, the only misclassification is a one-step ahead pre-alarm, which is acceptable from an operational safety and product quality viewpoint. In other words, the developed online drill condition detection system is exceedingly reliable.
4. The values of initial weights, learning rates, and smoothing factors influence the performance of the online drill detection system. Various values have been tested in order to achieve a very high reliability for the online drill condition detection system.
5. The drill sizes and drilling condition during the online tests were very different from those in the learning process. This indicates that neural networks have shown the capability of generalization. Therefore, the developed online drill condition detection system is very robust and can be utilized in very complex manufacturing environments. In summary, this research contributes greatly to the occupational safety of the drilling operation.

REFERENCES

Altintas, Y. (1992). Prediction of cutting forces and tool breakage in milling from feed drive current measurements. *ASME Journal of Engineering for Industry, 114*, 386–392.

Barker, R.W., Klutke, G., & Hinich, M.J. (1993). Monitoring rotating tool wear using higher-order spectral features. *ASME Journal of Engineering for Industry,* 115, 23–29.

Etherton, J.R., & Myers, M.L. (1990). Machine safety research at NIOSH and the future directions. *International Journal of Industrial Ergonomics, 6,* 163–174.

Govekar, E., & Grabec, I. (1994). Self-organizing neural network application to drill wear classification. *ASME Journal of Engineering for Industry, 116*(2), 233–238.

He, W., Zhang, Y.F., Lee, K.S., & Liu, T.I. (2001). Development of a fuzzy-neuro system for parameter resetting of injection molding. *ASME Journal of Manufacturing Science and Engineering, 123*, 110–118.

Kumagai, A., Hozian P., & Kirkland M. (2000). Neuro-fuzzy model based feedback controller for shape memory alloy actuator. In *Proceedings of SPIE's 7th Annual International Symposium on Smart Structures and Materials, Newport Beach, California* (pp. 291–299). Bellingham, WA, USA: Society of Photo-Optical Instrumentation Engineer (SPIE).

Li, G.S., Lau, W.S., & Zhang, Y.Z. (1992). In-process drill wear and breakage monitoring for a machining center based on cutting force parameters. *International Journal of Machine Tools and Manufacture—Design, Research and Application, 32*(6), 855–867.

Liu, T.I.. (1998). Tools for intelligent manufacturing process and systems: Neural networks, fuzzy logic, and expert systems. In *The CRC Handbook of Mechanical Engineering* (pp.13-98–13-102). New York, NY, USA: CRC Press.

Liu, T.I., & Anantharaman, K.S. (1994). Intelligent classification and measurement of drill wear. *ASME Journal of Engineering for Industry, 116*, 392–397.

Liu, T.I., Chen, W.Y., & Anantharaman, K.S. (1998). Intelligent detection of drill wear. *Journal of Mechanical Systems and Signal Processing, 12*(6), 863–873.

Liu, T.I., Chen, W.Y., & Ko, E.J. (1994). Intelligent recognition of drill wear states. *ASM Journal of Materials Engineering and Performance, 3*(4), 490–495.

Liu, T.I.., Lee, J., & Wang, Y.C. (2001). On-line monitoring of boring tools using virtual instrumentation and neural networks. In *Proceedings of the 6th International Conference on Manufacturing Technology, Hong Kong* (pp. 1–5). Hong Kong: Sino Electronic Publishing.

Liu, T.I., Wang, Y.C., & Lee, J. (2000). Predictive monitoring for precision boring of titanium parts. In *Proceedings of the NSF Workshop on Intelligent Maintenance Systems, Milwaukee, Wisconsin, USA, November 16–17, 2000* (pp. 1–27). Milwaukee, WI, USA: NSF Center for Intelligent Maintenance Systems.

Millard, D.L. (1991). Toward a reliable safety sensor implementation for industrial automation. *International Journal of Industrial Ergonomics, 7*, 277–286.

National Safety Council. (1992). *Accident prevention manual for business and industry— Engineering and technology* (10th ed.). Itasca, IL, USA: Author.

National Safety Workplace Institute (NSWI). (1992). *Basic information on workplace safety and health in the United States including a state by state analysis and profile*. Chicago, IL, USA: Author.

Niu, Y.M., Wong, Y.S., Hong, G.S., & Liu, T.I. (1998). Multi-category classification of tool conditions using wavelet packets and ART2 network. *ASME Journal of Manufacturing Science and Engineering, 120*, 807–816.

Park, J.J., & Ulsoy, A.G. (1993a). On-line flank wear estimation using an adaptive observer and computer vision, part 1: Theory. *ASME Journal of Engineering for Industry, 115*, 30–36.

Park, J.J., & Ulsoy, A.G. (1993b). On-line flank wear estimation using an adaptive observer and computer vision, part 2: Experiment. *ASME Journal of Engineering for Industry, 115*, 37–43.

Purushothaman, S., & Srinivasa, Y.G., (1994). A back propagation algorithm applied to tool wear monitoring. *International Journal of Machine Tools and Manufacture—Design, Research and Application, 34*(5), 625–631.

Ramamurthi, K., & Hough, C.L., Jr. (1993). Intelligent real-time predictive diagnostics for cutting tools and supervisory control of machining operations. *ASME Journal of Engineering for Industry, 115*, 268–277.

Rangwala, S., & Dornfeld, D. (1990). Sensor integration using neural networks for intelligent tool condition monitoring. *ASME Journal of Engineering for Industry, 112*, 219–228.

Roth, J.T., & Pandit, S.M. (1999). Monitoring end-mill wear and predicting tool fracture using accelerometers. *ASME Journal of Manufacturing Science and Engineering, 121*, 559–567.

Sata, T., Matsushima, K., Nagakura, T., & Kono, E. (1973). Learning and recognition of the cutting states by the spectrum analysis. *Annals of the CIRP, 22*(1), 41–42.

Sereno, M.E. (1993). *Neural computation of pattern motion-modeling stages of motion analysis in the primate visual cortex*. Cambridge, MA, USA: MIT Press.

Society of Manufacturing Engineers. (1976). *Tools and manufacturing engineers handbook* (Vol. 1, Machining, 4th ed.). Dearborn, MI, USA: Author.

Society of Manufacturing Engineers. (1984). *Fundamentals of tool design* (2nd ed.). Dearborn, MI, USA: Author.

Subramanian, K., & Cook, N.H. (1977). Sensing of drill wear and prediction of drill life. *ASME Journal of Engineering for Industry, 103*, 295–301.

Thangaraj, A., & Wright, P.K. (1988). Computer-assisted prediction of drill-failure using in-process measurements of thrust force. *ASME Journal of Engineering for Industry, 110*(2), 192–200.

Xie, Q., Bayoumi, A.E., & Kendall, L.A. (1990). On tool wear and its effect on machined surface integrity. *ASM Journal of Materials Shaping Technology, 8*(4), 255–265.